Available online at www.sciencedirect.com

ScienceDirect

Procedia Engineering 172 (2017) 338 – 346

Procedia Engineering

www.elsevier.com/locate/procedia

Modern Building Materials, Structures and Techniques, MBMST 2016

Strain Capacity of Reinforced Concrete Members Subjected to Uniaxial Tension

Lars German Hagsten[a]*, Annette Beedholm Rasmussen[a], Jakob Fisker[a]

[a]*Aarhus University, School of Engineering, 8000 Aarhus C, Denmark*

Abstract

The aim of this paper is to set up a method to determine the strain capacity of tension bars of reinforced concrete (RC) subjected to pure tension. Due to the interaction between reinforcement and concrete and due to the presence of cracks, the stresses in both reinforcement and concrete are varying along the length of the tension bar. The strain capacity of the tension bar is seen as the average strain in the reinforcement at the load level corresponding to the ultimate stress capacity of the reinforcement at the cracks. The result of the approach is in overall good agreement when comparing with 24 tests.

Peer-review under responsibility of the organizing committee of MBMST 2016

Keywords: Reinforced concrete, strain capacity, tension bar, crack patterns, crack spacings.

1. Introduction

Figure 1 illustrates the stress-strain curve for both a reinforcement bar and a tension bar. The reinforcement is modelled as bilinear. The stress-strain curve for the tension bar is sketched as a dotted line. This is due to the fact that the presented method only aims to estimate the strain capacity, and not the stress-strain relation from the stress free state to the ultimate state. The strain capacity of the tension bar is affected by a number of factors. In order to determine the strain capacity it is not important to know the exact stress/strain level at which the individual factors becomes dominant but only to know in which order they becomes dominant.

* Corresponding author. Tel.: +45-41 89 32 05.
E-mail address: lgh@ase.au.dk

Peer-review under responsibility of the organizing committee of MBMST 2016
doi:10.1016/j.proeng.2017.02.038

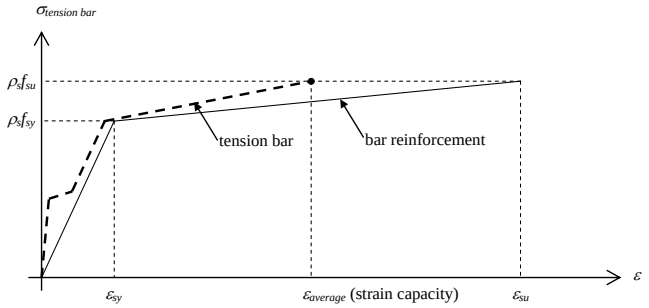

Fig. 1. Modelled stress strain curve for reinforcement together with principle relation for a tension bar.

The modelling can be split into three overall subtopics, that is:

a) determination of the crack distances
b) bond behavior locally at the cracks where minor conical cracks are formed. Hereby is formed a minor zone where there is no, or almost no, contact between concrete and reinforcement. The reinforcement is debonded in this area
c) bond between reinforcement and concrete at larger distances away from the cracks. That is outside the zone of the minor conical cracks

Concerning the later subtopic Fernandez *et al.* [1] has proposed analytical expressions for the modeling of the strain in the steel as function of the distances from cracks which convincible agree with experimental results by Shima *et al*. [2]. The analytical expressions are based on simple physical relations combined with non-linear FEM modelling. The test setup used by Shima *et al.* [2] is shown in Figure 2a. As can be seen in the figure a slip free zone with a length of $10\varnothing$ has been used to avoid the local effects. In Figure 2b is shown the relation between the measured shear stress (relative to $f_c^{2/3}$) as function of the ratio between the slip (S) and diameter of the reinforcement (in this figure denoted as "D"). The higher shear stress level (S/D < ≈7% in Figure 2b) represent the shear stress applicable for the reinforcement being in the elastic range, and the lower shear stress level represent the shear stress applicable for the reinforcement being in the plastic range. The FEM modelling by Fernandez et al indicates that the primary reason for the drop in shear stress are due to the transverse contraction of the reinforcement (as a v. Mise material the volume of the reinforcement is constant in yielding).

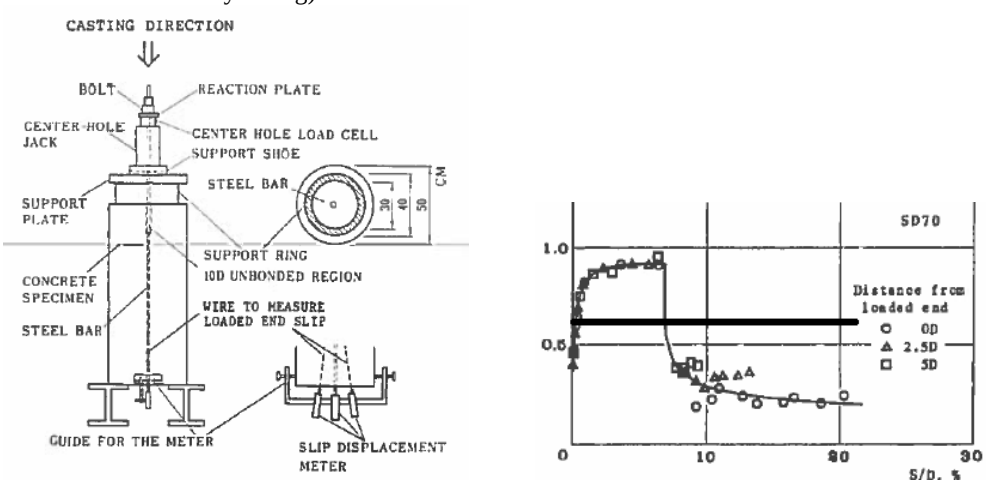

a b

Fig. 2. (a) test setup, [2] (b) bond strength as function of the relative displacement [1], [2].

Concerning the determination of the crack distances this can be done be means of simple equilibrium, combined with the strength of concrete in tension and modified with a statistical factor.

Goto [3] reported experiments in which small conical cracks were formed in the "neighborhood" of the primary cracks, see Figure 3a. Fernandez *et al.* have also set up an empirical expression to take this effect into account. The empirical expression has been compared with tests reported by Shima *et al*. [2] on beam elements, see Figure 3b. As it can been seen in the figure, this expression seems to underestimate the effect of the local debonding. It will be seen in this paper that the extension of this debonded zone plays an important role in determining the strain capacity. The strain intensity estimated by the model is not capturing the measured strain variation adjacent to the cracks. The measurements indicate that the local effects at the cracks are larger than modelled.

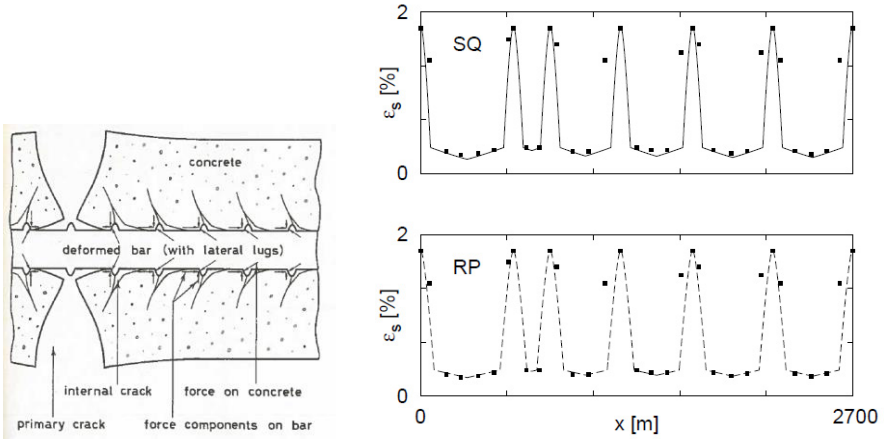

Fig. 3. (a) conical internal cracks [3] (b) strain distribution in reinforcement in beams [2].

2. Model

2.1. Formation of the stable stage of primary cracks

A tension bar, which is uncracked at the unloaded stage, is regarded. At a certain load level visible cracks with an orientation approximate perpendicular to the longitudinal direction is formed. These cracks are named primary cracks. The order in which they form is arbitrary. These cracks will be formed at different load levels prior to yielding. No more cracks will form when the distance between them has reached a certain low value, where the force which can be transferred between concrete and reinforcement is smaller than the force necessary to create more cracks. The crack pattern (concerning the primary cracks) has thus become stable. The average distance between the cracks is denoted s_{rm}.

In the following it is assumed that the cracked tension bar has a constant crack distance of s_{rm}. Hereby the tension bar is modelled as a bar with a periodic systems of cracks, where only one crack and a length equal to half of the distance between two cracks needs to be considered.

Based on the test performed by Shima et al., see Figure 2, it seems reasonable to argue that the shear stress between reinforcement and concrete is almost constant for small displacements. This constant level is valid up to a stress state at which the reinforcement starts to yield. As also seen in Figure 2 the shear stress decreases for larger displacements. This support the argument that the primary cracks are formed at a load level below yielding and that the shear stress relevant in determining the crack distance is the previously mentioned constant value. As it is indicated in Figure 2 this shear stress can be set to $\tau = 0.6 f_c^{2/3}$, where f_c is the compressive strength of the concrete.

This is in accordance with what has been proposed by Marti *et al.* [4]. The minimum distance between two cracks is determined by having the shear transfer over this distance to equalize the tensile capacity of the concrete:

$$s_{rm,\min} n\tau O = \left(A_c - nA_s\right) f_{ct} \tag{1}$$

$$s_{rm,\min} = \frac{\varnothing}{4}\frac{\left(A_c - nA_s\right)}{nA_s}\frac{f_{ct}}{\tau} = \frac{\varnothing}{4}\frac{\left(1-\rho_s\right)}{\rho_s}\frac{f_{ct}}{\tau} \tag{2}$$

$\varnothing$ is the diameter of the reinforcement, n is the numbers of reinforcement bars, A_s the area of one reinforcement bars, A_c is the cross sectional area of the tension bar and f_{ct} is the tensile strength of the concrete and can be expressed by $f_{ct} = 0.3 f_c^{2/3}$. By comparing the expression for τ and f_{ct} it can be seen that $\tau = 2f_{ct}$. The maximum distance between the cracks is given by $s_{rm,max} = 2s_{rm,min}$. The ratio between the minimum distance and the average distance has been studied by various researchers, and slightly different values have been found. In the following a value of 1.33 is used [5], [6]. The average distance is thus given by:

$$s_{rm} = 1.33\frac{\varnothing}{8}\frac{\left(1-\rho_s\right)}{\rho_s} \tag{3}$$

2.2. Shear stress/bond stress

The transfer of forces between reinforcement and concrete takes place locally at the ribs, but due to the closely placed ribs, the transfer is modelled as distributed shear stress. Fernandez *et al*. [1] found that the bond can be expresses as a basic bond strength, τ_s, multiplied with a bond coefficient, K_b, which primarily is affected by the contraction of the reinforcement.

$$\tau\left(\delta, \varepsilon_s, x\right) = \tau_s\left(\delta\right) \cdot K_b\left(\varepsilon_s\right) \tag{4}$$

Having the expression for τ, the strain in the reinforcement can be set up. Two different models have been presented by Fernadez et al. That is the Spuare Root Model and the Rigid-Plastic Model. The best compliance with test is found for the Square Root Model.

Square Root Model:

$$\varepsilon_s = \begin{cases} \varepsilon_{bu} - \left(\varepsilon_{bu} - \varepsilon_y\right)\exp\left(\dfrac{4 \cdot \tau_{b,\max}\left(x - l_p\right)}{E_h \cdot \phi_s \cdot \left(\varepsilon_{bu} - \varepsilon_y\right)}\right) & x \le l_p \\ \left(\sqrt{\varepsilon_y} - \dfrac{2 \cdot \tau_{b,\max} \cdot \left(x - l_p\right)}{E_s \cdot \phi_s \cdot \sqrt{\varepsilon_y}}\right)^2 & x > l_p \end{cases} \tag{5}$$

$\tau_{b,\max} = f_c^{2/3}$ and $\varepsilon_{bu} = 4a/\phi_s$.

The extension of the zone at which the reinforcement is yielding can be found directly using the above expression for ε_s in the case of $x = 0$ and $\varepsilon_s = \varepsilon_{s,o}$:

$$l_p = -\ln\left(\frac{\varepsilon_{s,o} - \varepsilon_{bu}}{\varepsilon_{bu} - \varepsilon_y}\right)\frac{E_h \cdot \phi_s \cdot \left(\varepsilon_{bu} - \varepsilon_y\right)}{4 \cdot \tau_{b,\max}} \tag{6}$$

2.3. Bond slip

At the load level at which the primary cracks are formed, small conical cracks propagate from the ribs of the reinforcement, see Figure 3a. These cracks are longest closest to the primary cracks and are inclined/oriented towards the primary cracks. As the stress level in the reinforcement is increased these small conical cracks increases further in length and numbers. The small conical cracks, which are located closest to the primary cracks will partly or fully reach the primary cracks, and thus partly or fully isolate the small, "triangular" area of the concrete from the remaining concrete. Thereby a zone in the "neighborhood" of the primary cracks, where no or almost no transfer between the reinforcement and the concrete can take place, see Figure 3a.

The length of this bond slip on each side of the crack can be given by the following expression, see [7].

$$l_{deb} = ½\left(1+\frac{\sigma_s}{100}\right)Ø \quad , \sigma_s \text{ in MPa} \tag{7}$$

σ_s is the stress in the reinforcement at a certain load level:

$$\sigma_s = \begin{cases} E_s\varepsilon_s & \varepsilon_s \le \varepsilon_y \\ f_y + E_h\left(\varepsilon_s - \varepsilon_y\right) & \varepsilon_s > \varepsilon_y \end{cases} \tag{8}$$

The formula for the debonded length on one side of the crack (l_{deb}) is on the same form as the formulas proposed by Jokela [8] and Leonhardt [9]. The formulas are empirical but show good agreement with an analytical expression for a punching analysis of the local effects, see figure 4.

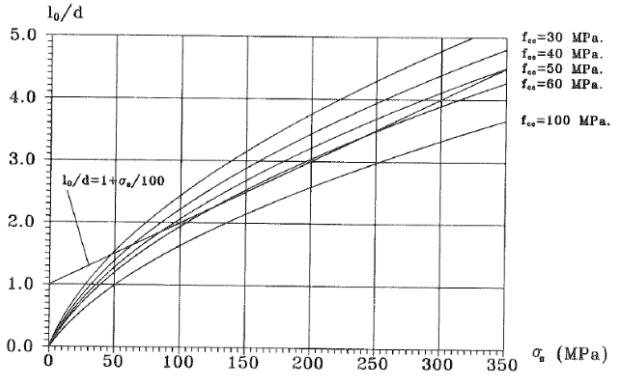

Fig. 4. Semi-empirical expression sketched together with theoretical determined curves [7]. $l_{deb} = ½l_o$.

The initial crack widths, which in some cases are large, can only be explained by the presence of such a debonded zone [9].

Fernandez et al has extended their model to also include this by multiplying the expression in (4) with a factor of $\lambda(x/\varnothing_s) \le 1$ on equation (4). λ seeks physically to cover the reduced shear transfer causes by the presence of the conical cracks.

$$\tau\left(\delta, \varepsilon_s, x\right) = \tau_s\left(\delta\right) \cdot K_b\left(\varepsilon_s\right) \cdot \lambda\left(x/\phi_s\right) \tag{9}$$

Where

$$\lambda\left(x/\phi_s\right)=1-\exp\left(\frac{-x}{\phi_s}\right) \tag{10}$$

The model by Fernandez et al $\lambda(x/\varnothing_s)$ is only attached to the post-yielding behavior. This is indicating that small conical cracks do only affect the behavior at post-yielding. This seems to be in contradiction to the observation of Shima et al and Leonhardt, and also in contradiction to the fact that the shear stress at that load level has decreased close to the primary cracks, whereby the ability to create small conical cracks must have vanished. Observations by Goto also show that the small conical cracks have been formed at a lower load level.

Model 1 (square root model including λ, [1]):

$$\varepsilon_s=\begin{cases}\varepsilon_{bu}-\left(\varepsilon_{bu}-\varepsilon_y\right)\exp\left[\dfrac{4\cdot\tau_{b,\max}}{E_h\cdot\phi_s\cdot\left(\varepsilon_{bu}-\varepsilon_y\right)}\left(\left(x-l_p\right)-\phi_s\cdot\left(\exp\left[-\dfrac{l_p}{\phi_s}\right]-\exp\left[-\dfrac{x}{\phi_s}\right]\right)\right)\right] & x\le l_p\\ \left(\sqrt{\varepsilon_y}-\dfrac{2\cdot\tau_{b,\max}\cdot\left(x-l_p\right)}{E_s\cdot\phi_s\cdot\sqrt{\varepsilon_y}}\right)^2 & x>l_p\end{cases} \tag{11}$$

Model 2 (square root model [1] with λ replaced by incorporation of l_{deb}):

$$l_p`=l_{deb}+l_p=l_{deb}-\ln\left(\frac{\varepsilon_{s,o}-\varepsilon_{bu}}{\varepsilon_{bu}-\varepsilon_y}\right)\frac{E_h\cdot\phi_s\cdot\left(\varepsilon_{bu}-\varepsilon_y\right)}{4\cdot\tau_{b,\max}} \tag{12}$$

$$\varepsilon_s=\begin{cases}\varepsilon_{s,o} & x\le l_{deb}\\ \varepsilon_{bu}-\left(\varepsilon_{bu}-\varepsilon_y\right)\exp\left(\dfrac{4\cdot\tau_{b,\max}\left(x-l_p`\right)}{E_h\cdot\phi_s\cdot\left(\varepsilon_{bu}-\varepsilon_y\right)}\right) & l_{deb}<x\le l_p`\\ \left(\sqrt{\varepsilon_y}-\dfrac{2\cdot\tau_{b,\max}\cdot\left(x-l_p`\right)}{E_s\cdot\phi_s\cdot\sqrt{\varepsilon_y}}\right)^2 & l_p`<x\end{cases} \tag{13}$$

3. Evaluation

The strain capacity is found as the average strain in the tension bar, which is identical to the average strain between two cracks:

$$\varepsilon_{capacity}=\varepsilon_{average}=\frac{1}{s_{rm}}\cdot 2\int_0^{\frac{1}{2}s_{rm}}\varepsilon_s\left(x\right)dx \tag{14}$$

Model 1 and model 2 has been compared with 24 tests [10]. These are characterized by f_c = 28.8 MPa, $f_{y,\varnothing10}$ = 558 MPa, $f_{u,\varnothing10}$ = 669 MPa, $E_{s,\varnothing10}$ = 192733 MPa, $\varepsilon_{u,\varnothing10}$ = 9.51%, $a_{\varnothing10}$ = 0.5 mm, $f_{y,\varnothing16}$ = 565 MPa, $f_{u,\varnothing16}$ = 676 MPa, $E_{s,\varnothing16}$ = 202230 MPa, $\varepsilon_{u,\varnothing16}$ = 11.3%, $a_{\varnothing16}$ = 1.0 mm. The comparison between the models and the tests is summarized in table 1. The comparison has been made based on both calculated and measured crack distances. It is seen that equation

(3) gives a reasonable accurate estimate of the crack distance for the specimens characterized with ρ_s equal to 1.29%, 1.40% and 3.57%, but a poor estimate for the specimens with ρ_s = 0.5%. The poor estimate for the low reinforcement degree could indicate that the bond stresses are higher for lower degrees of reinforcement. This is in accordance with the finding by Kaklauskas *et al.* [11].

By comparing model 1 and 2 with the tests it is seen that the best correlation is found for model 2.

In Figure 5 the calculated strain distribution in the reinforcement is shown for specimens 01-15. The calculated strain capacity found by equation (14) is shown by the dotted line. As seen in table 1, model 1 underestimates the strain capacity by 36% while model 2 in this case overestimates the strain capacity by 10%. The underestimation of the effects of the small conical cracks, reported by Shima et al, in model 1, is also seen in the modelling of the tested beams.

Table 1. Comparison between models and tests.

Specimen	Ø [mm]	A_s [mm^2]	ρ_s [%]	$s_{rm,calc.}$ [mm]	$\varepsilon_{average,calc.}/\varepsilon_{Model1}$	$\varepsilon_{average,calc.}/\varepsilon_{Model2}$	$s_{rm,meas.}$ [mm]	$\varepsilon_{average,meas.}/\varepsilon_{Model1}$	$\varepsilon_{average,meas.}/\varepsilon_{Model2}$
Spe01-15	10	75x75	1.40	117	1.56	0.90	113	1.50	0.89
Spe16-18	10	125x125	0.50	329	3.64	1.96	181	2.08	1.11
Spe19-21	16	75x75	3.57	72	1.00	0.90	93	1.06	0.90
Spe22-24	16	125x125	1.29	204	1.84	1.00	199	1.79	0.99
Average					2.01	1.19		1.61	0.97
Std.					114%	52%		44%	10%

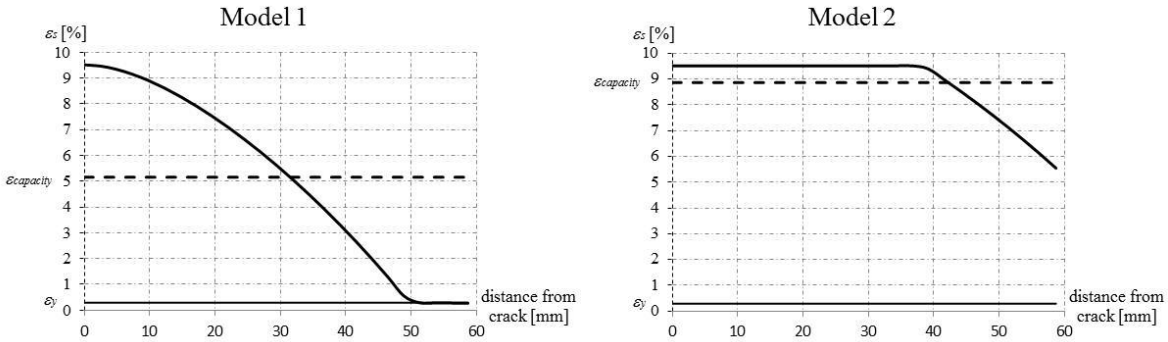

Fig. 5. Modelled steel strain distribution at ultimate load for model 1 and model 2. Spe01-15.

4. Strain capacity

Figure 6 illustrates the strain capacity for reinforcement of class A, B and C. The strain capacity is shown as function of ρ_s. Parameters used: f_c = 30 MPa, f_y = 500 MPa, a = 0.5 mm, A_c = 100 x 100 mm^2.

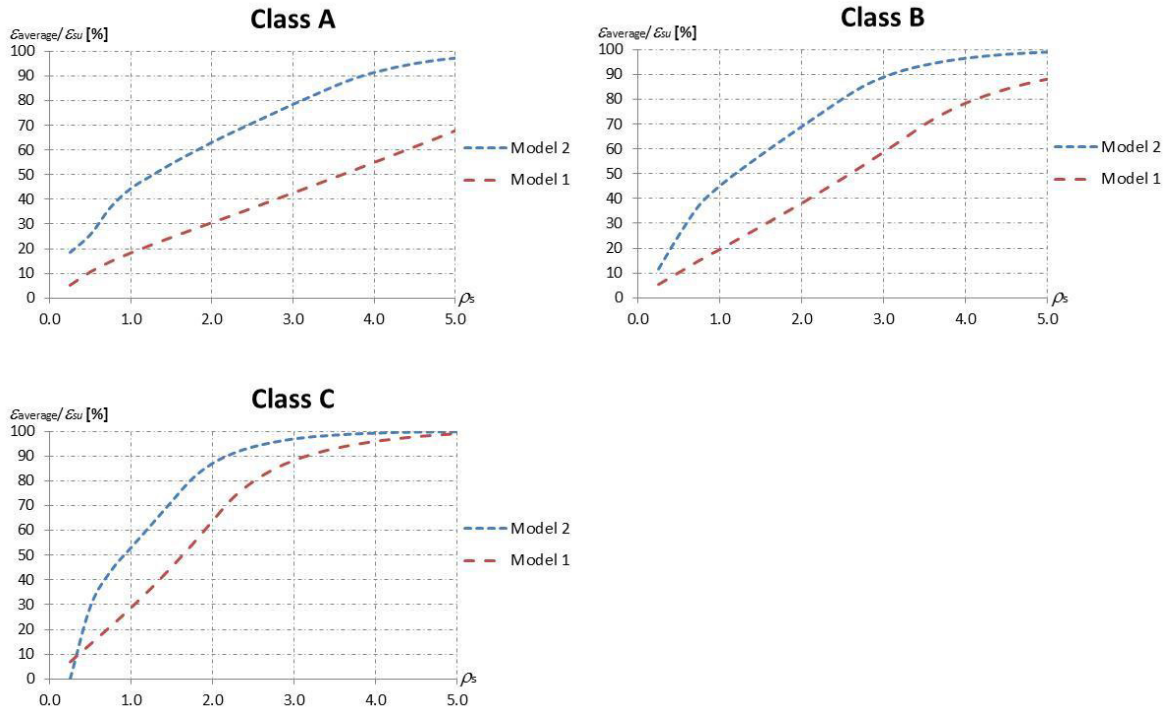

Fig. 6. Relative strain capacity as function of the degree of reinforcement for class A, B and C (classes according to EC2 [12]).

5. Discussion

In order to determine the strain capacity of reinforced concrete members subjected to uniaxial tension, existing models for the determination of cracks distances and variation of the strains in the reinforcement has been combined. The model for determination of crack distances seems to be reasonable accurate for the tests with higher degree of reinforcement, but rather poor for smaller degrees of reinforcement. An exixting model for the determination of the variation of the strains in the reinforcement seems to capture all important factors, but do also seem to underestimate the influence of small conical cracks. Therefor the part of the model, taking into account the influence of small conical cracks close to the primary cracks, has been replaced by another exiting model for the extension of the debonded zone at the cracks. Good correlation has been found when compared with 24 tests.

References

[1] Ruiz M. Fernandéz, A. Muttoni, P. Gambarova, Analytical modelling of the pre- and post-yield behavior of bond in reinforced concrete, ASCE Journal of Structural Engineering 133(10) (2007) 1364-1372.
[2] H. Shima, L–L. Chou and H. Okamura, Micro and macro models for bond in reinforced concrete, Journal of the Faculty of Engineering University of Tokyo XXXIX(2) (1887) 133–194.
[3] Y Goto, Cracks Formed in Concrete Around Deformed Tension Bars, ACI Journal 68(4 April) (1971) 244-251.
[4] P. Marti, M. Alvarez, W. Kaufmann, V. Sigrist, Tension Chord Model for Structural Concrete, Structural Engineering International, IABSE 8(4(1 November)) (1998) 287-298.
[5] R. Park and T.Paulay, Reinforced Concrete Structures, John Wiley & Sons, New York, 1975.
[6] S. H. Rizkalla and , L. S. Hwang, Crack prediction for members in uniaxial tension, ACI Journal 82(6 November–December) (1984) 572–579.
[7] D. H. Olsen, M. P. Nielsen, New theory to the determination of crack distances and crack widths in concrete structures (in Danish), serie R, No. 254, Department of Structural Engineering, Technical University of Denmark, 1989, pp. 1-145.
[8] J. Jokela, Dimensioning of Strain or Deformation – Controlled Reinforced Concrete Beams, Technical Research Centre of Finland. Publication 33. 1986.

[9] F. Leonhardt, Crack Control in Concrete Structures, IABSE Surveys, No 1, 1977
[10] Peter Drechsler Poulsen, Troels Primdahl, Bond Behaviour in Reinforced Concrete with Focus on Tension Stiffening in the Post-Yield Range. Master thesis, 2013, Aarhus University.
[11] Gintaris Kaklauskas, Viktor Gribniak, Ronaldas Jakubovskis, Eugenijus Gudonis, Donatas Salys & Rimantas Kupliauskas, Serviceability Analysis of Flexural Reinforced Concrete Members, Journal of Civil Engineering and Management 2012.
[12] EN-1992-1-1, Eurocode 2 – Design of Concrete Structures. Part 1–1: General Rules and Rules for Buildings, CEN, 2008.

Nomenclature

a	rib height	x	distance from crack
D	bar diameter	ε_{bu}	bond ultimate strain
E_s	elastic modulus of reinforcement	ε_y	yield strain of reinforcement
E_h	hardening modulus of reinforcement	ε_s	strain in reinforcement
f_c	compression strength of concrete	$\varepsilon_{s,o}$	strain in reinforcement at cracks
f_{ct}	tensile strength of concrete	ε_u	ultimate strain of reinforcement
f_y	yield strength of reinforcement	$\varepsilon_{capacity}$	strain capacity of RC tension member
f_u	ultimate strength of reinforcement	λ	reduction factor related to small conical cracks
k_b	bond coefficient	δ	relative bar – concrete slip
l_{deb}	debonded length	ρ_s	geometrical degree of reinforcement
l_p, l_p`	extension of plastic zone	τ_{max}	maximum bond stress
s_{rm}	crack distance	$\varnothing$	bar diameter
$s_{rm,min}$	minimum crack distance		